THE ASTROPHYSICAL JOURNAL, 619:L15–L18, 2005 January 20

THE ULTRAVIOLET GALAXY LUMINOSITY FUNCTION IN THE LOCAL UNIVERSE FROM *GALEX* DATA

TED K. WYDER,[1] MARIE A. TREYER,[1,2] BRUNO MILLIARD,[2] DAVID SCHIMINOVICH,[1,3] STÉPHANE ARNOUTS,[2] TAMÁS BUDAVÁRI,[4] TOM A. BARLOW,[1] LUCIANA BIANCHI,[5] YONG-IK BYUN,[6] JOSÉ DONAS,[2] KARL FORSTER,[1] PETER G. FRIEDMAN,[1] TIMOTHY M. HECKMAN,[4] PATRICK N. JELINSKY,[7] YOUNG-WOOK LEE,[6] BARRY F. MADORE,[8] ROGER F. MALINA,[2] D. CHRISTOPHER MARTIN,[1] PATRICK MORRISSEY,[1] SUSAN G. NEFF,[9] R. MICHAEL RICH,[10] OSWALD H. W. SIEGMUND,[7] TODD SMALL,[1] ALEX S. SZALAY,[4] AND BARRY Y. WELSH[7]

Received 2004 May 5; accepted 2004 July 27; published 2005 January 17

ABSTRACT

We present the results of a determination of the galaxy luminosity function at ultraviolet wavelengths at redshifts of $z = 0.0$–0.1 from *Galaxy Evolution Explorer* (*GALEX*) data. We determined the luminosity function in the *GALEX* far-UV and near-UV bands from a sample of galaxies with UV magnitudes between 17 and 20 that are drawn from a total of 56.73 deg^2 of *GALEX* fields overlapping the b_J-selected Two-Degree Field Galaxy Redshift Survey. The resulting luminosity functions are fainter than previous UV estimates and result in total UV luminosity densities of $10^{25.55\pm0.12}$ and $10^{25.72\pm0.12}$ ergs s^{-1} Hz^{-1} Mpc^{-3} at 1530 and 2310 Å, respectively. This corresponds to a local star formation rate density in agreement with previous estimates made with Hα-selected data for reasonable assumptions about the UV extinction.

Subject headings: galaxies: luminosity function, mass function — surveys — ultraviolet: galaxies

1. INTRODUCTION

In the past few years determinations of the star formation history of the universe have allowed us to begin to understand quantitatively when and how the stars in the universe were formed. Measurements of the rest-frame ultraviolet luminosities of galaxies have been particularly useful in this endeavor. In the very local universe, there is a relative lack of systematic surveys of galaxies in the UV. Before the launch of the *Galaxy Evolution Explorer* (*GALEX*), the most comprehensive survey of galaxies in the local universe was from the FOCA experiment (Milliard et al. 1992), a balloon-borne telescope that made measurements in a single band centered at 2000 Å. Based on FOCA observations of a total of ~2.2 deg^2, Treyer et al. (1998) and Sullivan et al. (2000) measured the first UV luminosity function (LF) for a sample of 273 galaxies with spectroscopic redshifts at $\bar{z} = 0.15$. Their LF has a steep, faint end slope and a total UV luminosity density (and corresponding star formation rate density) larger than most previous estimates. This higher local UV luminosity density in conjunction with measurements at larger distances led Wilson et al. (2002) to infer a luminosity density evolution proportional to $(1 + z)^{1.7\pm1.0}$, a trend shallower than had been estimated previously from the Canada-France Redshift Survey sample (Lilly et al. 1996).

In this Letter we present the first results regarding the UV LF based on measurements from *GALEX* in conjunction with redshifts from the Two-Degree Field Galaxy Redshift Survey (2dFGRS; Colless et al. 2001). The new *GALEX* data allow us to expand on the previous FOCA results using a much larger sample drawn from an area of 56.73 deg^2 but to a shallower limiting magnitude of $m_{\rm UV} = 20$. Throughout this Letter, we assume $H_0 = 70$ km s^{-1} Mpc^{-1}, $\Omega_M = 0.3$, and $\Omega_\Lambda = 0.7$.

2. DATA

The data analyzed in this Letter consist of 133 *GALEX* All-sky Imaging Survey (AIS) pointings that overlap the 2dFGRS in the south Galactic pole region. The *GALEX* field of view is circular, with a diameter of 1°.2, and each pointing is imaged simultaneously in both the far-UV (FUV) and near-UV (NUV) bands with effective wavelengths of 1530 and 2310 Å, respectively. The median exposure time for the fields is 105 s, allowing us to reach a signal-to-noise ratio of ~5 for FUV ≈ 20.0 and NUV ≈ 20.5. See Martin et al. (2005) and Morrissey et al. (2005) for details regarding the *GALEX* instruments and mission.

Sources were detected and measured from the *GALEX* images using the program SExtractor (Bertin & Arnouts 1996). As the NUV images are substantially deeper than the FUV images, we used the NUV images for detection and measured the FUV flux in the same aperture as for the NUV. The fields analyzed here were processed using a larger SExtractor deblending parameter, DEBLEND_MINCONT, because the standard *GALEX* pipeline processing tends to break well-resolved galaxies into more than one source. We elected to use the MAG_AUTO magnitudes measured by SExtractor through an elliptical aperture whose semimajor axis is scaled to 2.5 times the first moment of the object's radial profile, as first suggested by Kron (1980). All of the apparent magnitudes were corrected for foreground extinction using the Schlegel et al. (1998) reddening maps and assuming the extinction law of Cardelli et al. (1989). The ratio of the extinction in the *GALEX* bands to the reddening $E(B - V)$ was calculated by averaging the extinction law over each *GALEX* bandpass, re-

[1] California Institute of Technology, MC 405-47, 1200 East California Boulevard, Pasadena, CA 91125; wyder@srl.caltech.edu.

[2] Laboratoire d'Astrophysique de Marseille, BP 8, Traverse du Siphon, 13376 Marseille Cedex 12, France.

[3] Department of Astronomy, Columbia University, MC 2457, 550 West 120th Street, New York, NY 10027.

[4] Department of Physics and Astronomy, Johns Hopkins University, Homewood Campus, Baltimore, MD 21218.

[5] Center for Astrophysical Sciences, Johns Hopkins University, 3400 North Charles Street, Baltimore, MD 21218.

[6] Center for Space Astrophysics, Yonsei University, Seoul 120-749, Korea.

[7] Space Sciences Laboratory, University of California, Berkeley, 601 Campbell Hall, Berkeley, CA 94720.

[8] Observatories of the Carnegie Institution of Washington, 813 Santa Barbara Street, Pasadena, CA 91101.

[9] Laboratory for Astronomy and Solar Physics, NASA Goddard Space Flight Center, Greenbelt, MD 20771.

[10] Department of Physics and Astronomy, University of California, Los Angeles, CA 90095.

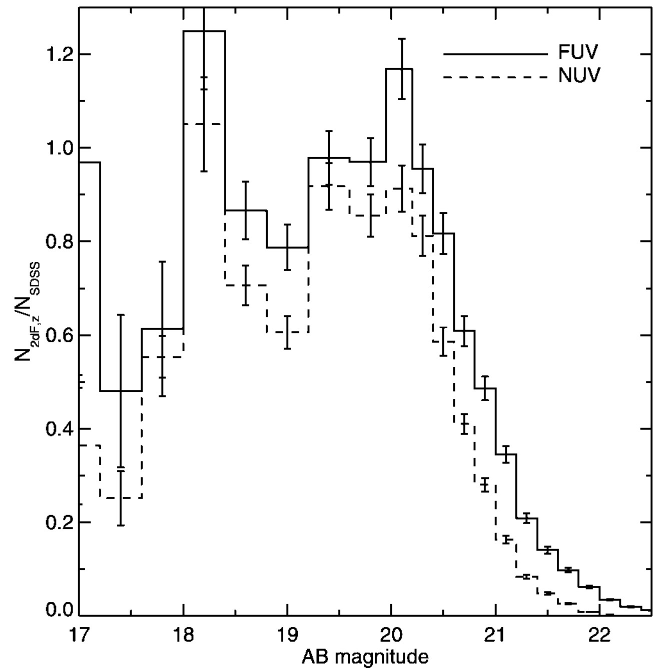

FIG. 1.—Completeness of the *GALEX*-2dF redshift sample defined as the ratio of the number counts of galaxies with 2dF redshifts to the number counts of galaxies as derived from *GALEX* observations that overlap the SDSS (Xu et al. 2005). The solid and dashed lines indicate the FUV and NUV redshift completeness, respectively.

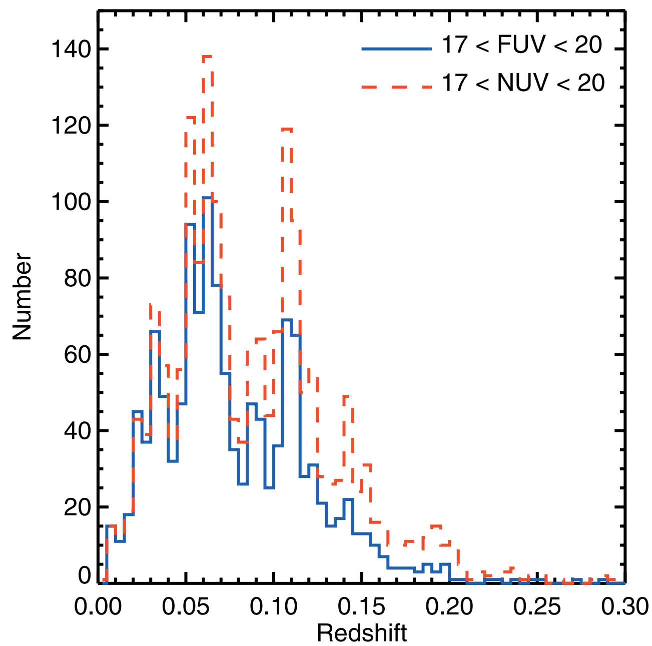

FIG. 2.—Redshift distributions of the FUV and NUV selected samples (*blue solid and red dashed lines, respectively*) in the range $17 \le m_{UV} \le 20$.

sulting in $A_{FUV}/E(B-V) = 8.376$ and $A_{NUV}/E(B-V) = 8.741$. The median extinction correction for the galaxies in our south Galactic pole sample is 0.15 mag in both bands, with the corrections ranging from 0.1 to 0.3 mag.

The *GALEX* catalogs were matched with the 2dFGRS input catalog using a search radius of 6″. To remove any overlap between adjacent pointings, we only included sources detected within the inner 0°.45 of each field. In addition, sources likely to be contaminated by artifacts from bright stars, with 2dF redshift quality flag less than three or with effective exposure times less than 60 s, were removed. Finally, we excluded *GALEX* sources in regions in which the 2dF redshift completeness was less than 80%. After applying all of these cuts to each band, the total area of *GALEX*-2dF overlap on the sky is 56.73 deg^2.

The *GALEX* resolution of 6″–7″ (FWHM) (Morrissey et al. 2005) is not sufficient to accurately separate stars and galaxies. Furthermore, the 2dFGRS input catalog, available from the 2dFGRS Web site,[11] only includes galaxies brighter than $b_J = 19.45$ and does not include stars. In order to assess the completeness of our 2dF-*GALEX* matched sample, we normalized our results to the total galaxy number counts determined by Xu et al. (2005) based primarily on 22.64 deg^2 of *GALEX* Medium Imaging Survey data overlapping the Sloan Digital Sky Survey (SDSS) Data Release 1 (Abazajian et al. 2003). As the SDSS data include stars and galaxies and reach fainter magnitudes, they result in a more accurate determination of the galaxy number counts in the UV. If we assume that the average galaxy number counts in the SDSS north Galactic pole fields are the same as those in the *GALEX*-2dF overlap, then the redshift completeness of the 2dF matched catalog is given by the number counts of galaxies with redshifts from 2dF divided by the total galaxy number counts from the SDSS overlap. This ratio is shown in Figure 1.

The completeness turns over at 20 mag because the redshift sample becomes incomplete for galaxies with blue (FUV $- b_J$) or (NUV $- b_J$) colors. We have limited our LF determination in each band to galaxies brighter than this limit. To avoid problems with photometry of large bright galaxies, we also imposed a bright magnitude limit of 17. The average completeness weighted by the number counts in the range 17–20 mag is 92% in the FUV and 79% in the NUV. For objects with magnitudes brighter than 20.0 in either band, we visually inspected all of the 2dF spectra and removed a total of 27 objects with very broad emission lines indicating that the objects are most likely some sort of active galactic nuclei. The redshift distributions for the FUV and NUV samples are shown in Figure 2.

We further restricted our sample to those galaxies with redshifts $z < 0.1$ to ensure that our sample is not sensitive to evolution. The average redshifts are 0.055 and 0.058 in the FUV and NUV, respectively. After applying all of the cuts mentioned in this section, a total of 896 galaxies in the FUV and 1124 galaxies in the NUV remained. The LFs for the objects with $z > 0.1$ are presented in Treyer et al. (2005).

3. LUMINOSITY FUNCTIONS

Using the FUV, NUV, and b_J magnitudes, we assigned a best-fit spectral type to each galaxy using a representative subset of the spectral energy distributions (SEDs) from Bruzual & Charlot (2003) and determined the *K*-correction needed to transform the observed UV magnitudes to rest-frame measurements at $z = 0$. The *K*-corrections are in general quite small ($\lesssim 0.2$).

We determined the LF $\Phi(M)$ and its error $\sigma[\Phi(M)]$ in each band using the V_{max} method (Felten 1976),

$$\Phi(M) = \sum f(m)/V_{max}, \quad (1)$$

[11] See http://www.mso.anu.edu.au/2dFGRS.

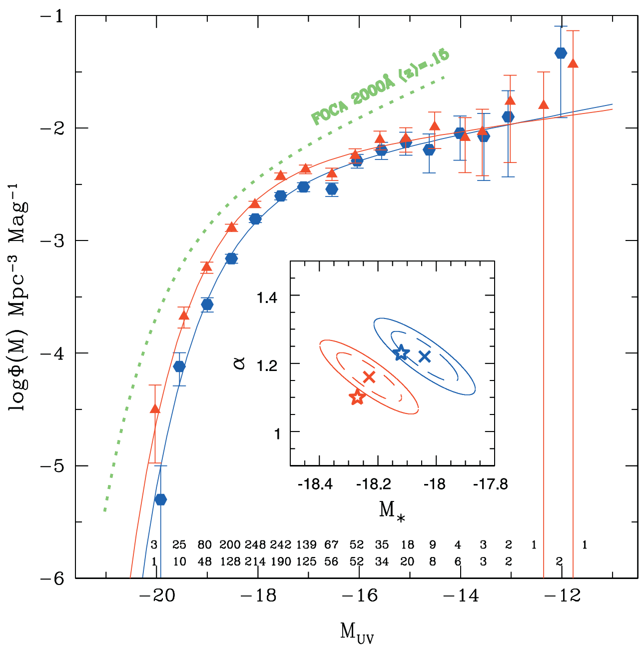

FIG. 3.—FUV (*blue circles*) and NUV (*red triangles*) LFs for $z < 0.1$. The solid lines are the Schechter function fits with best-fit parameters from Table 1. The dotted green line shows the LF measured at 2000 Å from FOCA data by Sullivan et al. (2000) over the range of absolute magnitudes explored in that study. The inset plots the 1 σ error contours of the Schechter function fits projected into the M^*-α plane for the FUV (*blue*) and NUV (*red*). The dashed contour shows values with $\chi^2 - \chi^2_{\rm min} = 1.0$, while the solid contour delineates $\chi^2 - \chi^2_{\rm min} = 2.3$, which corresponds to the joint 1 σ uncertainty on M^* and α. The red and blue stars indicate the best-fit values of M^* and α obtained from the STY method.

$$\sigma[\Phi(M)] = \left[\sum f^2(m)/V_{\rm max}^2\right]^{1/2}, \quad (2)$$

where $f(m)$ is the inverse of the redshift completeness as estimated in § 2 above and $V_{\rm max}$ is the maximum comoving volume within which each galaxy could have been observed given the bright and faint limiting magnitudes of our sample and its best-fit SED. The resulting LFs are shown in Figure 3.

By minimizing χ^2, we fitted the $V_{\rm max}$ LF points in each band with a Schechter function (Schechter 1976), $\Phi(L)dL = \phi^*(L/L^*)^\alpha e^{-L/L^*}\,dL/L^*$, where ϕ^*, M^*, and α were free parameters. The best-fit parameters and their errors, calculated using the range of solutions within 1.0 of the minimum χ^2, are listed in Table 1 along with the best-fit LF from Sullivan et al. (2000) converted to the AB magnitude system and to $H_0 = 70$. The errors in α and M^* are highly correlated, and the inset of Figure 3 shows the 1 σ error contours projected into the M^*-α plane. Since the $V_{\rm max}$ method can be biased in the presence of clustering, we also computed the best-fit Schechter parameters using the maximum likelihood STY method (Sandage et al. 1979). The resulting STY values are listed in Table 1 and are also plotted in the inset of Figure 3. The STY values lie just inside and outside the 1 σ $V_{\rm max}$ error ellipses in the FUV and NUV, respectively. We adopt the $V_{\rm max}$ results in § 4.

4. DISCUSSION

As can be seen in Figure 3, there are significant differences between the results presented here and those from Sullivan et al. (2000). The *GALEX* results have a fainter M^* in both bands and a shallower faint end slope. The FOCA passband is centered at 2015 Å with FWHM of 188 Å; thus, one would expect the FOCA results to lie between the *GALEX* FUV and NUV data. However, the FOCA sample is truly a UV-selected sample, while that presented here relies on the b_J-selected 2dFGRS. This selection could introduce a bias in our results if the galaxies for which we do not have redshifts have a different redshift distribution than the galaxies that are included in our sample. On the other hand, it is now well established that the UV luminosity density increases with redshift (e.g., Somerville et al. 2001), and part of the difference is likely a real effect (Treyer et al. 2005). However, the difference of ~0.9 mag between the FOCA and NUV values for M^* would require evolution much larger than that determined from other surveys, as well as *GALEX* data at higher redshifts (Arnouts et al. 2005; Schiminovich et al. 2005). A preliminary comparison of the *GALEX* and FOCA photometry in a couple of overlapping fields indicates that the FOCA magnitudes are on average brighter, with the difference becoming larger for fainter sources. It appears likely that these offsets and nonlinearities in the FOCA photometry account for a major part of the difference between the FOCA and *GALEX* LFs, with the remainder likely due to a combination of galaxy evolution and the FOCA sample selection.

In Table 1 we also list the total luminosity density calculated from the best-fit Schechter parameters as $\rho_L = \int_0^\infty L\Phi(L)dL = \phi^* L^* \Gamma(\alpha + 2)$. The statistical errors in log ρ_L that take into account the covariance between the three Schechter function parameters are 0.02 in each band. In addition to this error, the uncertainty in the *GALEX* photometric zero point is ≈10% in both bands, corresponding to an uncertainty in log ρ_L of 0.04. A potentially larger source of error is that due to large-scale structure. The variation in the number density of galaxies $\bar{n}$ in a contiguous volume V is given approximately by $\delta\bar{n}/\bar{n} \approx (J_3/V)^{1/2}$ (Davis & Huchra 1982), where J_3 is an integral over the galaxy two-point correlation function and has a value of $\sim 10^4$ Mpc^3 for a correlation function of the form $\xi(r) = (r/r_0)^{-\gamma}$ with $r_0 = 7.21$ Mpc and $\gamma = 1.67$ (Hawkins et al. 2003). The galaxy number counts from Xu et al. (2005) used to set the normalization of our LFs were derived from approximately 22.64 deg^2. For $z < 0.1$, the corresponding rms variation in the number density would be $\delta n/n \approx 0.24$, or an uncertainty in δ log $\rho_L \approx 0.11$. Since UV-selected, star-forming galaxies are likely less clustered than optically selected sam-

TABLE 1
SCHECHTER FUNCTION PARAMETERS

		$V_{\rm max}$ METHOD				STY METHOD	
BAND	z	M^*	α	log ϕ^* (Mpc^{-3})	log ρ_L (ergs s^{-1} Hz^{-1} Mpc^{-3})	M^*	α
FUV	0–0.1	−18.04 ± 0.11	−1.22 ± 0.07	−2.37 ± 0.06	25.55 ± 0.12	−18.12	−1.23
NUV	0–0.1	−18.23 ± 0.11	−1.16 ± 0.07	−2.26 ± 0.06	25.72 ± 0.12	−18.27	−1.10
FOCA	0.15	−19.10 ± 0.13	−1.51 ± 0.10	−2.48 ± 0.11	26.06 ± 0.15	…	…

ples, this value is really an upper limit. Adding these uncertainties due to large-scale structure and calibration in quadrature to the statistical errors results in a total uncertainty of $\delta \log \rho_L \approx 0.12$ in both bands.

The spectral slope β, defined as $f_\lambda \propto \lambda^\beta$ with f_λ in units of ergs s^{-1} Å^{-1} Mpc^{-3}, corresponding to our two luminosity density measurements is $\beta \approx -1.1$. This is slightly bluer than the slope of $\beta = -0.9$ determined by Cowie et al. (1999) at $z = 0.7$–1.3 from measurements at longer rest-frame wavelengths spanning 1700–2750 Å.

The FUV luminosity density can be used to estimate the star formation rate (SFR) density in the local universe. For a constant star formation history and a Salpeter initial mass function, the SFR is related to the UV luminosity L_ν (in the range 1500–2800 Å) by $\mathrm{SFR}(M_\odot\ \mathrm{yr}^{-1}) = 1.4 \times 10^{-28} L_\nu(\mathrm{ergs\ s^{-1}\ Hz^{-1}})$ (Kennicutt 1998). For the FUV luminosity density in Table 1, we obtain $\log \mathrm{SFR}_{\mathrm{FUV}}(M_\odot\ \mathrm{yr}^{-1}\ \mathrm{Mpc}^{-3}) = -2.30 \pm 0.12$ with no extinction correction. For comparison, the extinction-corrected Hα LF at $z \lesssim 0.045$ from Gallego et al. (1995) shifted to our assumed Hubble constant corresponds to $\log \mathrm{SFR}_{\mathrm{H}\alpha} = -1.86 \pm 0.04$ using the Hα-to-SFR conversion from Kennicutt (1998). Based on Hα imaging of a subsample of the galaxies used by Gallego et al. (1995), Pérez-González et al. (2003) argued that the local Hα luminosity density is ~60% higher because of uncertainties in the aperture corrections applied to the spectroscopic data and corresponds to $\log \mathrm{SFR}_{\mathrm{H}\alpha} = -1.6 \pm 0.2$. Bringing the FUV SFR into agreement with this result would require an extinction of $A_{\mathrm{FUV}} \simeq 1.8$.

An average extinction of $A_{\mathrm{FUV}} \simeq 1.8$ is consistent with a simple estimate made using the observed (FUV − NUV) colors. While there is a well-defined relationship between the UV extinction and the spectral slope for starburst galaxies, more quiescent galaxies tend to have less extinction for a given UV slope than would be inferred from nearby starbursts (Bell 2002). In particular, Kong et al. (2004) used the population synthesis models of Bruzual & Charlot (2003) along with the prescription described in Charlot & Fall (2000) for determining how starlight is absorbed by dust in galaxies to show that the smaller extinction in nonstarburst galaxies can be explained by variations in the galaxies' star formation histories. Based on a set of Monte Carlo realizations of these models spanning a range of extinctions, ages, and star formation histories, Kong et al. (2004) were able to approximate the dependence of the FUV extinction on the UV spectral slope β with the formula $A_{\mathrm{FUV}} = 3.87 + 1.87(\beta + 0.40 \log b)$, where the variable b parameterizes the star formation history and is defined as the ratio of current-to-past average SFR. Assuming a constant star formation history ($b = 1$), an extinction of $A_{\mathrm{FUV}} = 1.8$ is obtained for a spectral slope $\beta = -1.1$, a value consistent with that measured from the FUV and NUV luminosity densities. On the other hand, the average (FUV − NUV) color of our FUV-selected sample is 0.14, corresponding to a spectral slope of $\beta = -1.67$. For this β and $b = 1$, the Kong et al. (2004) formula results in $A_{\mathrm{FUV}} = 0.7$ mag. This extinction is similar to the results of Buat et al. (2005), who found that the average extinction for a local NUV-selected sample is $A_{\mathrm{FUV}} \simeq 1$ mag based on the far-IR to UV flux ratio. If an extinction of $A_{\mathrm{FUV}} \simeq 1$ is more appropriate for the UV-selected sample presented here, then the UV-based SFR density would be $\log \mathrm{SFR}_{\mathrm{FUV}} = -1.9 \pm 0.1$, a value lower than that from Hα but still consistent to within the errors. In reality, the extinction is likely a function of absolute magnitude, and future *GALEX* papers will address in more detail correcting UV fluxes for extinction in a more rigorous way.

In the near future we will continue our investigation of the UV LF in the local universe using *GALEX* AIS data covering ~1000 deg^2 of the SDSS. In addition to expanding our sample to include more galaxies, we will use the SDSS photometry and spectroscopy to explore the dependence of UV luminosity on other galaxy characteristics, such as color, surface brightness, environment, metallicity, and stellar mass.

GALEX (*Galaxy Evolution Explorer*) is a NASA Small Explorer launched in 2003 April. We gratefully acknowledge NASA's support for construction, operation, and science analysis for the *GALEX* mission, developed in cooperation with the Centre National d'Etudes Spatiales of France and the Korean Ministry of Science and Technology.

REFERENCES

Abazajian, K., et al. 2003, AJ, 126, 2081
Arnouts, S., et al. 2005, ApJ, 619, L43
Bell, E. F. 2002, ApJ, 577, 150
Bertin, E., & Arnouts, S. 1996, A&AS, 117, 393
Bruzual, G., & Charlot, S. 2003, MNRAS, 344, 1000
Buat, V., et al. 2005, ApJ, 619, L51
Cardelli, J. A., Clayton, G. C., & Mathis, J. S. 1989, ApJ, 345, 245
Charlot, S., & Fall, S. M. 2000, ApJ, 539, 718
Colless, M., et al. 2001, MNRAS, 328, 1039
Cowie, L. L., Songaila, A., & Barger, A. J. 1999, AJ, 118, 603
Davis, M., & Huchra, J. 1982, ApJ, 254, 437
Felten, J. E. 1976, ApJ, 207, 700
Gallego, J., Zamorano, J., Aragón-Salamanca, A., & Rego, M. 1995, ApJ, 455, L1
Hawkins, E., et al. 2003, MNRAS, 346, 78
Kennicutt, R. C., Jr. 1998, ARA&A, 36, 189
Kong, X., Charlot, S., Brinchman, J., & Fall, S. M. 2004, MNRAS, 349, 769
Kron, R. G. 1980, ApJS, 43, 305
Lilly, S. J., Le Fèvre, O., Hammer, F., & Crampton, D. 1996, ApJ, 460, L1
Martin, D. C., et al. 2005, ApJ, 619, L1
Milliard, B., Donas, J., Laget, M., Armand, C., & Vuillemin, A. 1992, A&A, 257, 24
Morrissey, P., et al. 2005, ApJ, 619, L7
Pérez-González, P. G., Zamorano, J., Gallego, J., Aragón-Salamanca, A., & Gil de Paz, A. 2003, ApJ, 591, 827
Sandage, A., Tammann, G. A., & Yahil, A. 1979, ApJ, 232, 352
Schechter, P. 1976, ApJ, 203, 297
Schiminovich, D., et al. 2005, ApJ, 619, L47
Schlegel, D. J., Finkbeiner, D. P., & David, M. 1998, ApJ, 500, 525
Somerville, R. S., Primack, J. R., & Faber, S. M. 2001, MNRAS, 320, 504
Sullivan, M., Treyer, M. A., Ellis, R. S., Bridges, T. J., Milliard, B., & Donas, J. 2000, MNRAS, 312, 442
Treyer, M. A., Ellis, R. S., Milliard, B., Donas, J., & Bridges, T. J. 1998, MNRAS, 300, 303
Treyer, M. A., et al. 2005, ApJ, 619, L19
Wilson, G., Cowie, L. L., Barger, A. J., & Burke, D. J. 2002, AJ, 124, 1258
Xu, C. K., et al. 2005, ApJ, 619, L11